

Towards establishing the spin of warped gravitons

Oleg Antipin*

*Department of Physics and Astronomy,
Iowa State University, Ames, IA 50011, USA*

Amarjit Soni†

*Brookhaven National Laboratory,
Upton, NY 11973, USA*

(Dated: October 24, 2018)

Abstract

We study the possibility of experimental verification of the spin=2 nature of the Kaluza-Klein (KK) graviton which is predicted to exist in the extra-dimensional Randall-Sundrum (RS) warped models. The couplings of these gravitons to the particles located on or near the TeV brane is the strongest as the overlap integral of their profiles in the extra-dimension is large. Among them are unphysical Higgses (W_L^\pm and Z_L) and KK excitations of the Standard Model (SM) gauge bosons. We consider the possibility to confirm the spin-2 nature of the first KK mode of the warped graviton (G_1) based on the angular distribution of the Z boson in the graviton rest frame in the $gg \rightarrow G_1 \rightarrow W^{KK}(Z^{KK})W(Z) \rightarrow WWZ$, $gg \rightarrow G_1 \rightarrow ZZ$ and $gg \rightarrow G_1 \rightarrow Z^{KK}Z \rightarrow ZZH$ decay channels. Using Wigner D-matrix properties, we derive the relationship between the graviton spin, signal angular distribution peak value, and other theoretically calculable quantities. We then study the LHC signals for these decay modes and find that with 1000 fb^{-1} of data, spin of the RS graviton up to $\sim 2 \text{ TeV}$ may be confirmed in the $pp \rightarrow W^{KK}(Z^{KK})W(Z) \rightarrow WWZ \rightarrow 3 \text{ leptons} + \text{jet} + \cancel{E}_T$ and $pp \rightarrow ZZ \rightarrow 4 \text{ leptons}$ decay modes.

*Electronic address: oaanti02@iastate.edu

†Electronic address: soni@bnl.gov

I. INTRODUCTION

With the upcoming start of the CERN LHC, our quest for the physics beyond SM is likely to yield positive results. On the theoretical side two of the most important questions to be answered are the Planck-weak hierarchy problem and the flavor puzzle of the SM. The Randall-Sundrum model with a warped extra dimension [1] is just about the only theoretical framework which simultaneously addresses both these questions making it a very compelling model of new physics. Perhaps the most distinctive feature of this scenario is the existence of KK gravitons with masses and couplings at the TeV scale which therefore should appear in experiment as widely separated resonances [2].

The original RS model as well as all of its extensions are based on a slice of AdS_5 space. At the endpoints of this five-dimensional space ($\phi = 0, \pi$), two branes are placed which are usually labeled as an ultraviolet (UV) Planck brane and an IR (TeV) brane; and the large hierarchy of scales is solved by a geometrical exponential factor. Postulating modest-sized 5th dimension with radius R and curvature k the TeV/Planck $\sim e^{-k\pi R}$ ratio of scales can be numerically obtained by setting $kR \approx 11$. In the original RS model all SM fields were localized on the TeV brane. The only new particles in this model were KK gravitons with no SM gauge quantum numbers. Later, in addition to the KK gravitons, a bulk scalar field with a ϕ -dependent vacuum expectation value (VEV) was shown to generate a potential to stabilize the R modulus [3]. However, this model leaves higher-dimensional operators in the 5D effective field theory suppressed only by TeV scale which, in turn, generates unacceptably large contributions to flavor changing neutral current (FCNC) and observables related to the SM electroweak precision tests (EWPT). A natural way to avoid this problem, proposed by [4, 5, 6, 7, 8], is to allow SM fields to propagate in the extra dimension. In this scenario there are KK excitations of SM gauge and fermion fields in addition to those of the graviton. These states have masses in the TeV range and are localized near the TeV brane. The SM particles are the zero-modes of the 5D fields, and the profile of a SM fermion in the extra dimension depends on its 5D mass. By localizing light fermions near the Planck brane and heavier ones near the TeV brane, the contributions to the FCNC and EWPT are suppressed by scales \gg TeV. As a consequence, the KK graviton whose profile is peaked at the TeV brane will couple mostly to the top quark, Higgs (or, by equivalence theorem, to the longitudinal W and Z bosons) [9, 10, 11], and KK excitations of the SM fields.

Thus, the promising channels to observe RS gravitons are those where produced gravitons are decaying to fields localized near TeV brane. The search for the KK gravitons using its decays to the top quarks was performed in [9]. Signals from graviton decay to W_L pair, which subsequently decay into pure leptonic or semileptonic final states, were considered in [12]. The 4-lepton signal through the decay to a pair of Z_L 's was studied in [10]. Reconstruction possibility of the Z 's via their leptonic decays makes this a uniquely clean mode.

In this paper we would like to address the issue of confirmation of the spin-2 nature of RS gravitons (for the most recent survey of methods of measuring the spin of new physics particles at the LHC, see [13]). The conventional way to measure the spin of a new particle involves reconstruction of its rest frame using its decay products and studying the angular distributions about the polarization axis. Along these lines, in [9] generic sample of a 100 $t\bar{t}$ events was produced for a spin-0, spin-1 and spin-2 resonances in an attempt to distinguish spin of the resonance based on the angular dependence of the cross-section. We, instead, concentrate on the $gg \rightarrow G_1 \rightarrow W^{KK}(Z^{KK})W_L(Z_L) \rightarrow ZZH, WWZ$ and $gg \rightarrow G_1 \rightarrow Z_L Z_L$ channels where, in addition to the $Z_L Z_L$ channel considered in the literature before, we have one KK partner of the W or Z and one longitudinally polarized W or Z in the final state. Due to W^{KK} and Z^{KK} presence in these new channels, invariant mass of their decay products should show resonant behavior. Reconstruction of these intermediate KK gauge bosons will be important to reveal the internal structure of the RS model. We will see that Z boson signal angular distribution in the graviton rest frame for all these modes peaks at 90 degrees to collision axis. Performing angular analysis using Wigner D-matrix, we will derive the relationship between the graviton spin, angular distribution peak value, and other theoretically calculable quantities. As our method only requires to measure this peak value, where most of the signal events will be concentrated, we may optimistically achieve this goal with a relatively low sample of $O(10)$ events.

II. MODEL

We closely follow the model discussed in [10] and briefly review it here. As discussed above, we allow SM fields to propagate in the extra-dimension and distribute fermions along it to generate observed mass spectrum without introducing additional hierarchies in the fundamental 5D theory. SM particles are identified with zero-modes of 5D fields, and the profile of the fermion in the extra dimension depends on its 5D mass. As was shown before [6, 7, 8], all fermion 5D masses are $O(1)$ parameters with the biggest one, among the SM quarks, being that of the top quark. To specify the model even further, the top quark is localized near the TeV brane and the right-handed isospin is gauged [14]. We consider t_R being on the TeV brane (see discussion of the other possibilities in [10], for example). At the end of the day, we are left with three parameters to be measured experimentally. We define them as $c \equiv k/M_{Pl}$ (the ratio of the AdS curvature k to the Planck mass), $\mu \equiv ke^{-\pi kR}$ monitors gauge KK masses with the first few being $(2.45, 5.57, 8.7\dots) \times \mu$, and finally the parameter $\nu \equiv m/k$ which defines where the lightest fermion with bulk mass m is localized. For the t_R on the TeV brane, $\nu_{t_R} \approx 0.5$; and parameters c and μ will remain free in our analysis.

A. Low energy constraints on model parameters

Before proceeding further, let us briefly review constraints placed on the warped extra-dimension model with custodial isospin symmetry [14], which we adopt in this paper. In the resulting setup of [14], KK mass scale as low as ~ 3 TeV is allowed by precision electroweak data. Regions of parameter space that successfully reproduce the fit to electroweak precision observables with KK excitations as light as ~ 3 TeV were also studied in [15]. Phenomenological consequences of the observed $B\bar{B}$ -mixing were discussed in [16]. In the model of [14] tree level exchange of KK gluons gives the dominant contribution to the $B\bar{B}$ -mixing. In [16], the CP-violating effects on the B_d system were shown to provide $M_{gluon}^{(1)} > 3.7$ TeV constraint at 68% CL.

Phenomenological constraints from lepton-flavor-violations were discussed in [17, 18]. In [17], “anarchic” Randall-Sundrum model of flavor was studied, and the minimal allowed KK scale of ~ 3 TeV was found to be permitted for a few points in the natural RS parameter space; but models with custodial isospin can relax these constraints. In [18], extensive analysis of $B \rightarrow K^* l^+ l'^-$ modes was performed, concluding that only the $B \rightarrow K^* ee$ decay have sizable new physics effects. With SM contributions being suppressed, current experimental bounds were translated into the lepton bulk mass parameters. For the first KK gauge boson mass of 2-4 TeV, 10-20% deviation from the SM results were found. Top quark flavor violations and B-factory signals were also studied in [19, 20, 21]. Finally, enhanced contributions to $\Delta S = 2$ processes generated by beyond the SM operators with $(V - A) \otimes (V + A)$ structure, present in these frameworks, may impose additional constraints [22]. Without further flavor structure these contributions were expected to place a lower bound on the KK gluon mass of $O(8 \text{ TeV})$ [23, 24]. However, most recent studies of the flavor constraints on the new physics mass scale find that the KK gluon mass should generically be heavier than about 21 TeV [25].

Relentless attempts to lower KK-mass scale further still flourish on the market. On this road, a number of other models were proposed trying to improve the prospects to discover KK-particles at the LHC. One of them is a model presented in [26] with a somewhat surprising claim that KK masses as low as 1 TeV are consistent with all current experimental constraints. An interesting variant of the warped extra dimension based on 5D minimal flavor violation was recently proposed in [27]. The model allows to eliminate current RS flavor and CP problem [19, 28] with a KK scale as low as 2 TeV. Closing the list of examples, a volume-truncated version of the RS scenario called “Little Randall-Sundrum (LRS)” model was constructed in [29]. With the assumption of separate gauge and flavor dynamics, this setup allows to suppress a number of unwanted contributions to precision electroweak, $Zb\bar{b}$, and flavor observables, compared with the corresponding RS case.

Summarizing, we may say that KK gauge bosons with masses below 3 TeV (which would imply $m_G \gtrsim 4$ TeV) would be difficult to have in current theoretical constructions. If this is the case, signals at the LHC, confirming the RS idea, would be extremely difficult to find; and studies conducted in [10, 24] and later in this

paper support this unfaored future. However, in view of the above discussion, it also seems plausible that these models are still being developed; and, therefore, it is not inconceivable that explicit construction(s) will be found which will allow KK masses lower than 3 TeV without conflict with electroweak precision experiments and/or with flavor physics. This attitude was taken in [30] and we in this paper will also adopt this point of view.

B. Couplings of KK gravitons

After these brief remarks we can write the couplings relevant to our discussions here. Since the graviton $h_{\mu\nu}$ couples to the energy-momentum tensor $T^{\mu\nu}$, coupling of the n th level KK graviton to the q th and m th level gauge bosons has the generic form:

$$L_G = \frac{C_{qmn}}{M_{Pl}} T^{\mu\nu(q,m)} h_{\mu\nu}^{(n)}, \quad (1)$$

where the magnitude of the C_{qmn} coupling constants depends on the overlap of the particle wavefunctions in the extra-dimension.

Analytic expressions for the coefficients C_{qmn} with the flat zeroth mode gauge boson profile may be found in [2] and for the W_L and Z_L on the TeV brane we need to replace them with delta functions. We present resulting couplings in Table I along with partial decay widths for dominant decay channels for the lightest KK ($n=1$) graviton which will be the focus of our analysis; see also [10]. The $W_L W_L, Z_L Z_L$ and hh decay channels illustrate equivalence theorem once again, which is valid up to $(m_{W,Z}/m_G)^2$ where m_G is the graviton mass.

Let us briefly explain the result for the $\Gamma(G_n \rightarrow W_{KK} W_L)$ decay mode as it involves off-diagonal elements of the energy-momentum tensor of the gauge fields. The gauge boson mass matrix is [17]:

$$\frac{m_W^2}{2} \sum_{m,n=0} a_{mn} A_\mu^{(m)} A^{\mu(n)}, \quad (2)$$

and for the TeV brane Higgs scenario the off-diagonal elements a_{0m} that describe the mixing of the zero and the m th KK mode $a_{0m} = \sqrt{2\pi k R}$. Thus, the off-diagonal elements of the energy-momentum tensor are given by:

$$T_{\mu\nu}^{W(m,0)} = \eta_{\mu\nu} \left\{ \frac{1}{2} F^{\rho\sigma(m)} F_{\rho\sigma}^{(0)} - m_W^2 \sqrt{2\pi k R} A^{\rho(m)} A_\rho^{(0)} \right\} - \left\{ F_\mu^{\rho(m)} F_{\nu\rho}^{(0)} + F_\mu^{\rho(0)} F_{\nu\rho}^{(m)} - m_W^2 \sqrt{2\pi k R} (A_\mu^{(m)} A_\nu^{(0)} + A_\mu^{(0)} A_\nu^{(m)}) \right\}. \quad (3)$$

To the leading order in the m_W/m_{KK} , this results in the partial decay rate:

$$\Gamma(G_n \rightarrow W_{KK} W_L) = \frac{(C_{W_L W_{KK} G})^2 m_{G_n}^3}{480\pi} \cdot \left(1 - \frac{m_{KK}^2}{m_{G_n}^2}\right) \cdot \frac{m_W^2}{m_{KK}^2} \cdot f\left(\frac{m_{KK}}{m_{G_n}}\right), \quad (4)$$

TABLE I: Couplings of the first level KK graviton to the SM fields. The t_R is assumed to be localized on the TeV brane. Parameter m_1^G is the mass of n=1 graviton, $x_1^G = 3.83$ is the first root of the first order Bessel function and $\epsilon \equiv e^{k\pi R}$. $N_c = 3$ is number of QCD colors.

SM fields	C_{qm1}	Partial decay widths for n=1 graviton
gg(gluons)	$\frac{\epsilon}{2\pi kR}$	negligible
$W_L W_L$	ϵ	$(cx_1^G)^2 m_1^G / 480\pi$
$Z_L Z_L$	ϵ	$(cx_1^G)^2 m_1^G / 960\pi$
$t_R \bar{t}_R$	ϵ	$N_c (cx_1^G)^2 m_1^G / 320\pi$
h h	ϵ	$(cx_1^G)^2 m_1^G / 960\pi$
$W^{KK} W_L$	ϵ	$390 (cx_1^G)^2 m_1^G / 960\pi \cdot (m_W / m_1^G)^2$
$Z^{KK} Z_L$	ϵ	$390 (cx_1^G)^2 m_1^G / 960\pi \cdot (m_Z / m_1^G)^2$

where $f(x) \equiv r^2 + (6r^2 + 20r + 6)x^2 + 14(2 - r^2)x^4 + (6r^2 - 20r + 6)x^6 + r^2x^8$, $r \equiv \sqrt{2\pi kR} \approx 8.4$, and we neglected W boson mass in the phase-space consideration.

In the class of models we are working with, $m_1^G \approx 1.5m_1^{KK}$ for the mass of the lightest KK graviton and the gauge fields [2] which translates into $f(2/3) \approx 173$. As graviton mass changes from 1.5 to 3 TeV (which will be the typical range for the graviton mass we consider in this paper), for our numerical estimates we take the $Br(G_1(2.25TeV) \rightarrow W_{KK}W_L) \approx Br(G_1(2.25TeV) \rightarrow Z_{KK}Z_L) \approx 1/2 \times Br(G_n \rightarrow Z_L Z_L)$.

The suppression in the coupling of the graviton to the gluons follows because the gauge boson has a flat wavefunction, and thus its couplings to the graviton is suppressed by the volume of the bulk $\pi kR \approx 35$. For the same reason, the decay of gravitons to transverse W and Z bosons, as well as photons, are suppressed by this volume factor. The masses of the KK gravitons are given by $m_n = x_n \mu$ where x_n is n'th zero of the first order Bessel function. Notice that we do not need $q\bar{q}G$ coupling as it is Yukawa-suppressed, and graviton production is dominated by gluon fusion.

In this model the total width of the graviton is found to be $\Gamma_G = \frac{14(cx_1^G)^2 m_1^G}{960\pi}$ which is split between 6 dominant decay modes to $W_L W_L$, $Z_L Z_L$, $t_R \bar{t}_R$, hh, $Z_{KK} Z_L$, and $W_{KK} W_L$ in the ratio 2:1:9:1:0.5:0.5. Taking $c \sim 1$, the total graviton width is $\sim 7\%$ of its mass and is very close to the corresponding width for RS KK Z' in the same model [24].

III. GRAVITON SPIN MEASUREMENT

Now we discuss the strategy to confirm the spin-2 nature of the first KK mode of the RS graviton in our channels. Out of five possible polarization states of the graviton gluons can produce only $|JJ_Z \rangle = |2 \pm 2 \rangle$ and $|JJ_Z \rangle = |20 \rangle$ states due to two facts: gluons do not have longitudinal polarizations and the total angular

momentum has to be equal to $J=2$ (where we have chosen beam axis to be in the z-direction). Now, suppose that the two gauge bosons from graviton decay are produced at the polar angle θ . We rotate the gluons-produced graviton state specified by polarization tensor $\epsilon_{\mu\nu}(JJ_Z)$ by this angle [31]:

$$\epsilon_{\mu\nu}(2J_Z) = \sum_{J'_Z} D_{J_Z J'_Z}^{(J)*}(0, \theta, 0) \epsilon'_{\mu\nu}(2J'_Z), \quad (5)$$

where $\epsilon_{\mu\nu}(JJ'_Z)$ is the graviton state with the z-axis along the direction of the decay products, and $D_{J_Z J'_Z}^{(J)}(\alpha, \theta, \gamma) \equiv \langle JJ'_Z | R(\alpha, \theta, \gamma) | JJ_Z \rangle = e^{-iJ'_Z \alpha} d_{J_Z J'_Z}^{(J)}(\theta) e^{-iJ_Z \gamma}$ is the Wigner D-matrix. Independent Wigner small d-matrix elements for the spin-2 state are presented in Appendix [32]. Now we may easily derive the angular dependence of the helicity amplitudes for our channels. They follow from Eq.5 for the $|2 \pm 2 \rangle$ graviton state which is produced by $|+- \rangle$ and $| - + \rangle$ gluons states:

$$\epsilon_{\mu\nu}(2 \pm 2) = d_{\pm 2 0}^{(2)}(\theta) \epsilon'_{\mu\nu}(20) + d_{\pm 2 1}^{(2)}(\theta) \epsilon'_{\mu\nu}(21) + d_{\pm 2 -1}^{(2)}(\theta) \epsilon'_{\mu\nu}(2-1). \quad (6)$$

Now just use Clebsch-Gordan decomposition of the $\epsilon'_{\mu\nu}(20)$ and $\epsilon'_{\mu\nu}(2 \pm 1)$ states in terms of $1 \otimes 1$ final spin states to observe that, for example, helicity amplitude $A[g(\lambda_1)g(\lambda_2) \rightarrow Z(\lambda_3)Z(\lambda_4)] \equiv A_{\lambda_1 \lambda_2 \lambda_3 \lambda_4}$ for $A_{+-00} \sim d_{20}^{(2)}(\cos\theta)$, $A_{+-0-} \sim d_{21}^{(2)}(\cos\theta)$, and $A_{+-0+} \sim d_{2-1}^{(2)}(\cos\theta)$, where we have used Z boson in the final state for concreteness. Notice that we have not included the $d_{\pm 2 2}^{(2)}(\theta) \epsilon'_{\mu\nu}(22)$ and $d_{\pm 2 -2}^{(2)}(\theta) \epsilon'_{\mu\nu}(2-2)$ terms in Eq.6 as W and Z from graviton decay have longitudinal polarization and, thus, these terms cannot contribute.

Why $\epsilon_{\mu\nu}(20)$ graviton state does not contribute? This is again due to the fact that a gluon is massless. If you allow a gluon to have mass, you will obtain additional helicity amplitudes proportional to the mass of the gluon in agreement with the above angular analysis. For example, someone would find that $A_{++00} \sim d_{00}^{(2)}(\cos\theta)$, $A_{++0+} \sim d_{0-1}^{(2)}(\cos\theta)$, etc.

Inherent to our analysis is the assumption that a graviton is produced essentially at rest so that its decay products are mostly back to back. The requirement to find the graviton center of mass frame will limit possible decay channels for the gauge bosons as we will see later. If the rest frame cannot be reconstructed, we need to look for Lorentz invariant angular correlations which would encode information on the spin of the intermediate resonance. We do not pursue this approach here.

Now we use the fact that the Wigner D-matrix elements $D_{mk}^j(\alpha, \beta, \gamma)$ form a complete set of orthogonal functions of the Euler angles α, β, γ (we use symbols j and J for the total angular momentum quantum number interchangeably):

$$\int_0^{2\pi} d\alpha \int_0^\pi \sin \beta d\beta \int_0^{2\pi} d\gamma D_{m'k'}^{j'}(\alpha, \beta, \gamma)^* D_{mk}^j(\alpha, \beta, \gamma) = \frac{8\pi^2}{2j+1} \delta_{m'm} \delta_{k'k} \delta_{j'j}, \quad (7)$$

to determine the spin of the resonance state.

Taking into account SM background events, we observe that measured normalized angular distribution is related to the graviton spin in the following way:

$$\frac{d\sigma}{\sigma d\cos\theta} = \frac{\sum_{i=0,\pm 1} C_i \times [d_{2i}^{(2)}(\cos\theta)]^2 + \sigma_{backgd}(\cos\theta)}{\frac{2}{2j+1} \sum_{i=0,\pm 1} C_i + \sigma_{backgd}}, \quad (8)$$

where we used the normalization for the Wigner small d-matrix, C_i 's are parton level cross section expansion coefficients convoluted over gluon PDF's, and we sum over three polarization states of the final state gauge bosons. As we will see for all the channels considered below, signal Z boson angular distribution peaks at pseudorapidity $\eta = 0$ and, consequently, we will apply Eq.8 at this point.

IV. APPLICATIONS

We estimated SM background with the aid of the COMPHEP package [33]. For our graviton signal we used Mathematica program and partially cross-checked them with COMPHEP. CTEQ5M PDF's were used throughout (in their Mathematica distribution package [34] as well as intrinsically called by COMPHEP).

A. ZZ decay channel

To see the method at work, let us start with the simplest example of $gg \rightarrow G_n \rightarrow Z_L Z_L \rightarrow e^+ e^-, \mu^+ \mu^-$ discussed in [10] where the distinctive 4-lepton signal allows the reconstruction of all the masses of the particles in the decay chain. The dominant SM background for this purely leptonic mode is the $pp \rightarrow ZZ + X$, and the clean four-charged-lepton signal makes this mode a “golden” one. For this process we have:

$$\begin{aligned} A_{+-00} &= A_{-+00} = \frac{s^2(\beta^2 - 2)\sin^2\theta}{2} = \sqrt{\frac{2}{3}}s^2(\beta^2 - 2)d_{\pm 20}^{(2)}(\cos\theta) \\ A_{++00} &= A_{--00} = 0, \end{aligned} \quad (9)$$

where $\beta = \sqrt{1 - 4M_Z^2/s}$ is the Z boson velocity.

Neglecting the SM background for a moment and using Eq.8, we find that:

$$\frac{d\sigma_{signal}}{\sigma_{signal} d\cos\theta} = \frac{2j+1}{2} d_{\pm 20}^{(2)}(\cos\theta) d_{\pm 20}^{(2)*}(\cos\theta) = \frac{5}{2} d_{\pm 20}^{(2)}(\cos\theta) d_{\pm 20}^{(2)*}(\cos\theta), \quad (10)$$

and, thus, the height of the peak in the normalized signal angular distribution as in Fig.1a is characteristic of the spin of the resonance. For our case, distribution peaks at $5/2 \times (\sqrt{6}/4)^2 = 15/16$ and is independent of the graviton mass.

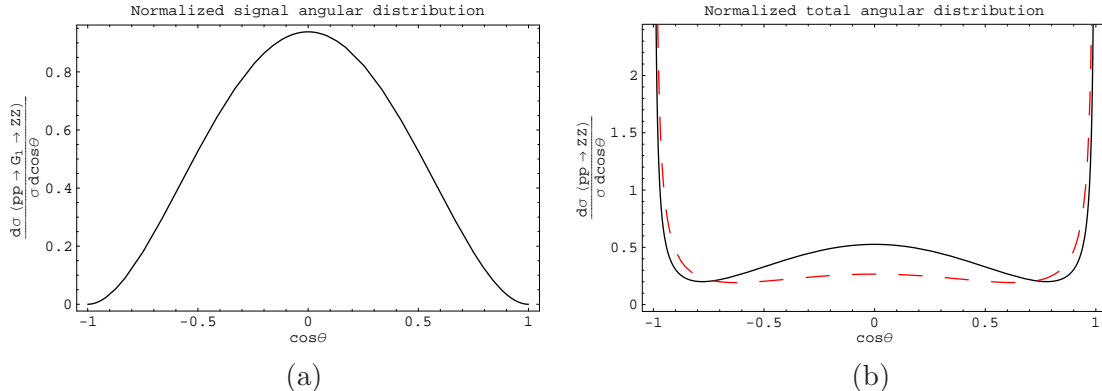


FIG. 1: (a) Normalized angular distribution for the signal $\sigma(pp \rightarrow G_1 \rightarrow ZZ)$ cross-section due to the 1st KK graviton mode and (b) Normalized total (i.e. including SM background) angular distribution for the $\sigma(pp \rightarrow ZZ)$ cross-section for $m_1^G = 1.5$ TeV (solid) and $m_1^G = 3$ TeV (dashed) integrated in the $m_1^G \pm \Gamma_G$ ZZ invariant mass window with $c \equiv k/M_{Pl} = 1$.

The irreducible SM background to the ZZ final state is dominated by $q\bar{q}$ annihilation as gluon fusion proceeds via loop and, thus, interference of the KK graviton signal with SM background is negligible. The background cross-section exhibits forward/backward peaking due to t/u channel exchange while KK signal concentrates in the central rapidity region[10].

On Fig.1b we show the total (signal plus background) cross-section integrated in the $m_1^G \pm \Gamma_G$ ZZ invariant mass window for two samples, 1.5 TeV and 3 TeV, graviton masses. For these mass values, we find SM background at $\cos\theta=0$ as $\sim 6\%$ and $\sim 23\%$ of the signal, respectively. We observe that for 1.5 TeV case peak value at $\cos\theta=0$ changed to ≈ 0.5 due to the fact that for this graviton mass $\sigma_{backgd} \approx \sigma_{signal}$ in $m_1^G \pm \Gamma_G$ ZZ invariant mass window [10] and, thus peak value reduced by \sim half after normalization (see also Table II). For the 3 TeV mass, the peak value ~ 0.2 as $\sigma_{backgd} \approx 3 \times \sigma_{signal}$. We may also impose pseudorapidity η cut to reduce background, keeping the signal (almost) unchanged. For example, for the $\eta < 2$ cut considered in [10], we find peak values as ~ 0.8 and ~ 0.5 for the 1.5 TeV and 3 TeV graviton masses respectively. Also, the background may be further reduced using lepton angular distribution to distinguish longitudinally polarized Z bosons from RS graviton decay from SM background [35].

Finally, using numerical results from Ref.[10] and including $Z \rightarrow \tau^+\tau^-$ channel not considered there, we obtain statistics presented in Table.II. We assume 100% efficiency for our clean 4-lepton signal. Poisson statistics CL to observe at least one signal event will be appropriate description if the number of background events $\lesssim 10$. We see that for 1.5 TeV and 3 TeV gravitons with 1000 fb^{-1} of data, we expect to have ~ 130 events and ~ 1 event respectively. This implies that higher luminosities are needed to reach 3 TeV graviton KK mass (for 3 ab^{-1} SLHC discussed in the community, see for example [36]). The reason for optimism on the issue of the detection of the τ 's from Z decay is that ~ 500 GeV energy τ 's have a decay length

TABLE II: Signal $pp \rightarrow ZZ \rightarrow 4$ leptons cross-section (in fb) for the $m_G = 1.5$ TeV and $m_G = 3$ TeV with the corresponding leading SM background. Numbers in brackets correspond to $\eta < 2$ cut case. For the low number of events, $\lesssim 10$, Poisson statistics is an appropriate description and the corresponding confidence level is, therefore, used. We assume 100% efficiency for our clean 4-lepton signal.

1.5 TeV	No cuts	$\eta < 2$ cut	# of events/1000 fb ⁻¹	S/B	S/ \sqrt{B}
Signal $G \rightarrow ZZ \rightarrow 4$ lept.	0.13	0.13	130	1.3(6.5)	13(29)
SM $ZZ \rightarrow 4$ lept.	0.1	0.02	100(20)		
3 TeV	No cuts	$\eta < 2$ cut	# of events/1000 fb ⁻¹	S/B	CL
Signal $G \rightarrow ZZ \rightarrow 4$ lept.	0.001	0.001	1	0.33(1.25)	57% (54%)
SM $ZZ \rightarrow 4$ lept.	0.003	0.0008	3(0.8)		

of $l = \gamma\tau c \approx 20$ mm and therefore might leave visible tracks in the detector [37].

B. $W^{KK}(Z^{KK})W_L(Z_L)$ decay channels

For our next examples we need to consider the matrix element for the $gg \rightarrow G_n \rightarrow W^{KK}(Z^{KK})W_L(Z_L)$ in the helicity basis. Working in the parton center of mass frame, the result is:

$$M(g^a g^b \rightarrow W_L W^{KK}) = \frac{c^2}{2\pi k R \mu^2} \cdot \frac{\sum_{\lambda_1, \lambda_2, \lambda_3, \lambda_4} A_{\lambda_1 \lambda_2 \lambda_3 \lambda_4} \delta_{ab}}{s - (m_n^G)^2 + i\Gamma_n^G m_n^G} \quad (11)$$

where helicity amplitudes relevant for our process are:

$$A_{+-00} = A_{-+00} = \frac{\{\sqrt{2\pi k R}((r^2 - 1)^2 m_W^4 - r^4 s^2) - 4r^2 s m_W^2\} \sin^2 \theta}{2r^3} \quad (12)$$

$$A_{+-0+} = A_{-+0+} = \sqrt{\frac{s}{2}} \frac{m_W}{r^2} \left\{ (\sqrt{2\pi k R} - 1) m_W^2 + (\sqrt{2\pi k R} + 1) r^2 s \right\} (1 - \cos \theta) \sin \theta$$

$$A_{+-0-} = A_{-+0-} = \sqrt{\frac{s}{2}} \frac{m_W}{r^2} \left\{ (\sqrt{2\pi k R} - 1) m_W^2 + (\sqrt{2\pi k R} + 1) r^2 s \right\} (1 + \cos \theta) \sin \theta$$

$$A_{++00} = A_{--00} = A_{++0+} = A_{++0-} = A_{--0+} = A_{--0-} = 0$$

with $r \equiv m_W/m_W^{KK}$. To obtain $M(g^a g^b \rightarrow Z_L Z^{KK})$ replace m_W with m_Z . We have checked our results with Ref.[35] where the process $gg \rightarrow G_n \rightarrow ZZ$ was considered (which translates into $r=1$ in our notation), and we confirmed them.

After straightforward calculation we arrive at the parton level cross-section:

$$\frac{d\sigma(gg \rightarrow W_L W^{KK})}{d\cos\theta} = \frac{|M|^2}{512\pi s} \left(1 - \frac{(m_W^{KK})^2}{s}\right), \quad (13)$$

TABLE III: Branching ratios of W' and Z' in the TeV brane Higgs scenario.

Decay modes	W'	Z'
$W_L H$	0.51	-
$W_L W_L$	-	0.35
$W_L Z_L$	0.40	-
$Z_L H$	-	0.60
$t\bar{t}$	-	0.05
tb	0.09	-

where we have neglected the W boson mass in the phase-space consideration.

As W^{KK} and Z^{KK} subsequently decay, we need to know their main decay channels which we now turn our attention to.

From now on, we generically call n th KK states of W and Z as W' and Z' . We consider the simplified single bulk $SU(2)_L$ case and take $(t, b)_L$ to have close to a flat profile and t_R on the TeV brane as they together do the best in satisfying the combined flavor-changing neutral currents (FCNC) and precision constraints. After that, the decay widths for the leading channels of Z' and W' are [24] :

$$\begin{aligned}
 \Gamma(W' \rightarrow tb) &= \frac{g_{SM}^2 m_{W'}}{16\pi}, & \Gamma(Z' \rightarrow t\bar{t}) &= \frac{g_{SM}^2 (\kappa_V^2 + \kappa_A^2) m_{Z'}}{4\pi c_w^2} \\
 \Gamma(W' \rightarrow W_L H) &= \frac{g_{SM}^2 \kappa^2 m_{W'}}{192\pi}, & \Gamma(Z' \rightarrow Z_L H) &= \frac{g_{SM}^2 \kappa^2 m_{Z'}}{192\pi c_w^2} \\
 \Gamma(W' \rightarrow W_L Z_L) &= \frac{g_{SM}^2 c_w^2 \kappa^2 m_{W'}}{192\pi}, & \Gamma(Z' \rightarrow W_L W_L) &= \frac{g_{SM}^2 c_w^2 \kappa^2 m_{Z'}}{192\pi},
 \end{aligned} \tag{14}$$

where in the TeV brane Higgs scenario $\kappa \equiv g_n/g_{SM} \approx \sqrt{2\pi k\bar{R}} \approx 8.4$ is the coupling strength of n th KK state relative to SM $SU(2)_L$ coupling, and $c_w(s_w)$ is the cosine (sine) of the Weinberg mixing angle. Notice that Ref.[24] assumed Higgs as A_5 [38, 39] and, thus, the IR brane coupling enhancement is equal to $\sqrt{\pi k\bar{R}}$ there. Also, using the values of $t\bar{t}Z'$ overlap integrals for the fermion profiles specified above [24], we obtain $\kappa_V \approx 1/4 - 5s_w^2/3$ and $\kappa_A \approx -1/4 - s_w^2$. The enhancement of SM coupling for the decay channels in the last two rows of Eq.14 follows from the fact that all the participating fields have a profile peaked near TeV brane compared to transverse zero-modes of W and Z , both having a flat profile in extra-dimension. Moreover, $W' \rightarrow tb$ decay channel is not enhanced since $(t, b)_L$ fields have a close to a flat profile. Corresponding branching fractions implied by Eq.14 are presented in Table III.

We focus only on the 1st KK mode of W and Z as the effects of heavier KK modes are suppressed. On Fig.2 we present the total resonant cross-section $\sigma(pp \rightarrow W_L W^{KK}) \approx \sigma(pp \rightarrow Z_L Z^{KK})$ integrated in the $m_1^G \pm \Gamma^G W_L W^{KK}$ mass window.

Using branching ratios in Table III total cross-sections after KK state decays may be easily obtained.

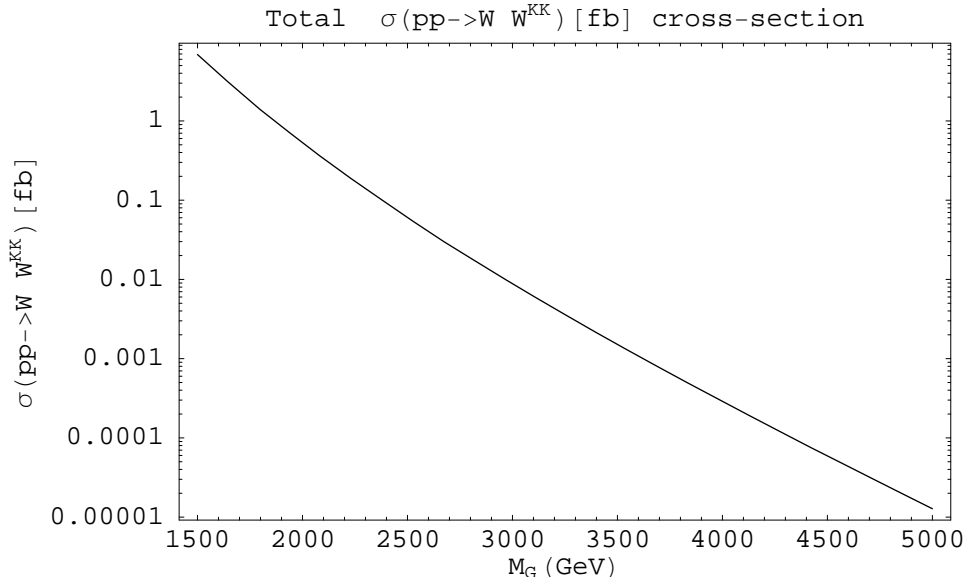


FIG. 2: (a) Total signal cross-section $\sigma(pp \rightarrow W_L W^{KK}) \approx \sigma(pp \rightarrow Z_L Z^{KK})$ as a function of the 1st KK graviton mode mass integrated in the $m_1^G \pm \Gamma^G W_L W^{KK}$ mass window and with $c=1$.

Thus, the five possible final states are: $W_L W_L Z_L$ (which may come from both $Z_L Z'$ and $W_L W'$ intermediate states), tbW_L , $t\bar{t}Z_L$, $W_L W_L H$, and $Z_L Z_L H$. In this paper we will concentrate on $W_L W_L Z_L$ and $Z_L Z_L H$ states. $W_L W_L H$ final state faces the challenge to reconstruct efficiently the W mass from the W decay products. We will not consider tbW_L and $t\bar{t}Z_L$ final states as both of them may additionally be produced through an s-channel KK gluon exchange which couples strongly to the $t\bar{t}$ pair.

ZZH decay channel

We are now in a position to discuss the more complicated case of the $pp \rightarrow G \rightarrow ZZ^{KK} \rightarrow ZZH$ final state where we have three independent helicity amplitudes involved (see Eq.12) compared to the above ZZ case where only one independent helicity amplitude survived. We assume that both Z's decay leptonically so that both Z masses can be reconstructed. Then, as one of the Z bosons comes directly from the graviton decay, it will have a bigger energy than the other one. We again would like to know how angular distribution of this Z may help to determine the spin of resonance its emitted from. We consider the ideal situation of pure signal events first and then add background events (which will depend on the mass of the Higgs) later.

Again writing $d\sigma_{signal}/d\cos\theta \equiv \sum_i C_i \times [d_{2i}^{(2)}(\cos\theta)]^2$ and using $C_1 = C_{-1}$, we have:

$$\frac{d\sigma_{signal}}{\sigma_{signal}d\cos\theta} = \frac{C_0 \times [d_{20}^{(2)}(\cos\theta)]^2 + C_1 \times ([d_{2-1}^{(2)}(\cos\theta)]^2 + [d_{21}^{(2)}(\cos\theta)]^2)}{\frac{2}{2j+1} \times (C_0 + 2C_1)}, \quad (15)$$

and, thus, the peak value occurs in this case at $\frac{(3/8C_0+C_1/2)}{\frac{2}{5}(C_0+2C_1)} \approx 0.77$. The normalized angular distribution is shown on Fig.3a and again is independent of the mass of the graviton. Obviously, Fig.3a applies to WWH and WWZ cases as well because the helicity amplitudes are the same.

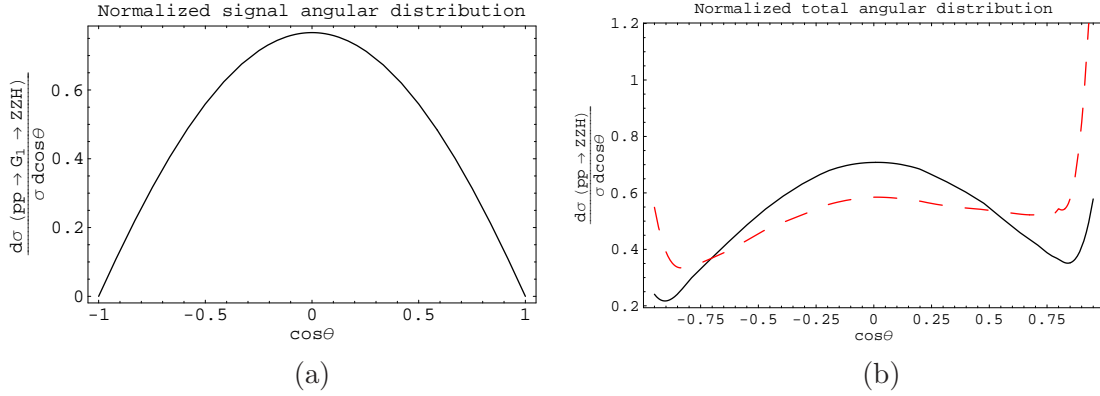


FIG. 3: (a) Normalized angular distribution for the signal $\sigma(pp \rightarrow G_1 \rightarrow ZZH)$ cross-section due to the 1st KK graviton mode and (b) Normalized total angular distribution for $m_1^G = 1.5$ TeV (solid) and $m_1^G = 2$ TeV (dashed) with cuts as in Eq.16.

Let us now consider the SM background for the ZZH case. It will depend on the leading decay mode(s) of the Higgs which, in turn, will depend on the mass of the Higgs boson. Important features can be highlighted by considering $m_H = 120$ GeV case for which the leading Higgs decay mode is $H \rightarrow b\bar{b}$. Due to the large Lorentz boost of the Higgs, we expect 2 b-jets to merge; and, thus, we conservatively require to have 4-leptons + 1 tagged b in the final state.

We consider 1.5 TeV and 2 TeV sample graviton masses and impose the following cuts:

$$\begin{aligned} m_G = 1.5 \text{ TeV} : & \quad |\eta_{Z,H}| < 2, \quad m_G - \Gamma_G < M_{ZZH} < m_G + \Gamma_G \\ m_G = 2 \text{ TeV} : & \quad |\eta_{Z,H}| < 2, \quad m_G - 2\Gamma_G < M_{ZZH} < m_G + 2\Gamma_G, \end{aligned} \quad (16)$$

where for 2 TeV case we doubled the ZZH invariant mass window to increase the number of events.

We use a b-tagging efficiency of 0.4 with a rejection factor for light jets (u, d, s, g) $R=20$ [40]. We use a charm rejection factor $R_c = 5$. In addition, we used $\text{BR}(H \rightarrow b\bar{b})=0.7$ and $\sum_{e,\mu,\tau} \text{BR}(Z \rightarrow \ell^+\ell^-) \approx 0.1$. All this results in the cross-sections presented in the second column of Table.IV. We find a clear signal above the background for 1.5 TeV case and 80% CL for 2 TeV case. Notice that we used the efficiency/rejection parameters optimized for low transverse momentum of the

TABLE IV: $pp \rightarrow ZZH \rightarrow 4$ leptons $b\bar{b}$ cross-section (in fb) for the signal with $m_G = 1.5$ TeV and $m_G = 2$ TeV and the corresponding leading SM backgrounds with cuts as in Eq.16 and efficiency/rejection factors as discussed in the text. For the low number of events, $\lesssim 10$, Poisson statistics is an appropriate description and the corresponding confidence level is, therefore, used.

1.5 TeV	Cuts and b-tag	# of events/500 fb ⁻¹	S/B	CL
Signal $G \rightarrow ZZH \rightarrow 4$ leptons + $b\bar{b}$	0.0196	9.82	6.7	99.9%
SM $ZZb \rightarrow 4$ leptons + b	1.6×10^{-4}	0.08		
SM $ZZq_\ell \rightarrow 4$ leptons + q_ℓ	1.5×10^{-3}	0.75		
SM $ZZg \rightarrow 4$ leptons + g	1.2×10^{-3}	0.6		
SM $ZZc \rightarrow 4$ leptons + c	5.6×10^{-5}	0.028		
2 TeV	Cuts and b-tag	# of events/1000 fb ⁻¹	S/B	CL
Signal $G \rightarrow ZZH \rightarrow 4$ leptons + $b\bar{b}$	1.82×10^{-3}	1.82	1.36	61%
SM $ZZb \rightarrow 4$ leptons + b	6.65×10^{-5}	6.65×10^{-2}		
SM $ZZq_\ell \rightarrow 4$ leptons + q_ℓ	5.24×10^{-4}	0.52		
SM $ZZg \rightarrow 4$ leptons + g	7.28×10^{-4}	0.73		
SM $ZZc \rightarrow 4$ leptons + c	2.41×10^{-5}	2.41×10^{-2}		

b-quark P_{Tb} , and rejection is expected to improve for high P_{Tb} which is the case at hand. Also, efficient reconstruction of Z mass from hadronic Z decay will increase the number of signal events as those modes have a bigger BR.

On Fig.3b. we show the normalized angular distributions for 1.5 TeV and 2 TeV graviton masses considered. We observe that for 1.5 TeV mass 0.77 peak value remains (almost) unchanged as the distribution is dominated by signal events, while for the 2 TeV mass value peak is less distinct.

WWZ decay channel

As discussed above, signal angular distribution is the same as in Fig.3a for this case because the helicity amplitudes are the same. Additionally, WZ or WW invariant mass presumably should have resonant (due to W' or Z') distribution; but we don't impose cuts on WZ or WW mass as we would like to keep our analysis as general as possible. At this point we have to decide on the decay modes of W and Z boson. We again allow Z decay leptonically so that we reconstruct Z mass efficiently, and we use the angular distribution of this Z for determination of the spin of the graviton. Now, if we allow both W 's decay hadronically, due to the huge Lorentz boosts of these W 's, we pick up 2 leptons + 2 jets as a background for our decay mode which we find to be overwhelmingly bigger than our signal. Thus, we use ($W \rightarrow jet$) ($W \rightarrow$ leptons) and ($Z \rightarrow$ leptons) as our final state.

For the leptonic W decay, due to small angular separation between missing

neutrino and charged lepton, we may estimate longitudinal (L) component of the ν 's momentum as:

$$p_\nu^L \approx \frac{\cancel{E}_T p_l^L}{p_{T_l}}. \quad (17)$$

Using this collinear approximation, the momentum of the leptonic W is reconstructed and, thus, we can calculate the (presumably) resonant invariant mass of the WW or WZ system. In doing so, we assumed that leptons are coming from the W decay as the reconstructed leptonic W mass will be zero in the collinear approximation. Also notice that in this approximation, the M_{WW} measurement error for the TeV energy W bosons is $\sim m_W/E_W \sim 0.1$.

We again consider 1.5 TeV and 2 TeV sample graviton masses and impose the following cuts:

$$|\eta_{Z,W}| < 1, \quad m_G - \Gamma_G < M_{WWZ} < m_G + \Gamma_G. \quad (18)$$

We have to remember that Eq.8 is valid only if we integrate over whole angular coverage of the detector. Fortunately, as our signal concentrates in central rapidity region, even such a hard pseudorapidity cut changed the signal cross-section for both graviton masses only by about 8% which is in the range of experimental uncertainties. This cut also changed the peak value in the normalized angular distribution of Fig.3a from 0.77 to 0.83 value.

In addition, we use the result of [24] which finds that jet mass cut:

$$65 \text{ GeV} < M_{jet} < 115 \text{ GeV} \quad (19)$$

achieves acceptance fraction of 0.78 for the signal and 0.3 for the background events. Table.V shows our results after all this cuts are imposed.

Finally, on Fig.4 we show the normalized angular distributions for the 1.5 TeV and the 2 TeV graviton masses considered. We observe that for the 1.5 TeV mass peak value of 0.83 for the case of zero background changed to about 0.7. This value can also be obtained applying Eq.8 and using the fact that for this mass $\sigma_{backgd} \approx \sigma_{signal}$ as can be seen in Table.V and the fact that $\sigma_{signal}(\cos\theta = 0) \approx 1.68\sigma_{backgd}(\cos\theta = 0)$. For the 2 TeV mass value, peak is no longer seen due to the dominance of the background.

V. CONCLUSIONS

In this work, we have extended earlier studies of the discovery potential of warped gravitons at the LHC which concentrated on the gravitons decaying into the ‘‘gold-plated’’ $Z_L Z_L$ channel, $W_L W_L$, channel and into the $t\bar{t}$ pair. We have considered resonant production of the first RS KK graviton mode via gluon-fusion process followed by its subsequent decay to $W^{KK}(Z^{KK})W_L(Z_L)$ and $Z_L Z_L$ pairs. We focused on confirmation of the unique spin-2 nature of the graviton using Z boson

TABLE V: $pp \rightarrow WWZ \rightarrow 3 \text{ leptons} + \text{jet} + \cancel{E}_T$ cross-section (in fb) for the signal with $m_G = 1.5 \text{ TeV}$ and $m_G = 2 \text{ TeV}$ and the corresponding leading SM backgrounds with cuts as in Eq.18 and Eq.19 and efficiency/rejection factors as discussed in the text.

1.5 TeV	Cuts	# of events/300 fb ⁻¹	S/B	S/ \sqrt{B}
Signal $G \rightarrow WWZ \rightarrow 3 \text{ leptons} + \text{jet} + \cancel{E}_T$	0.10	30	1.16	5.9
SM $WWZ \rightarrow 3 \text{ leptons} + \text{jet} + \cancel{E}_T$	0.0026	0.78		
SM $WZq \rightarrow 3 \text{ leptons} + \text{jet} + \cancel{E}_T$	0.0656	19.7		
SM $WZg \rightarrow 3 \text{ leptons} + \text{jet} + \cancel{E}_T$	0.018	5.4		
2 TeV	Cuts	# of events/1000 fb ⁻¹	S/B	S/ \sqrt{B}
Signal $G \rightarrow WWZ \rightarrow 3 \text{ leptons} + \text{jet} + \cancel{E}_T$	0.008	8	0.26	1.44
SM $WWZ \rightarrow 3 \text{ leptons} + \text{jet} + \cancel{E}_T$	6.8×10^{-4}	0.68		
SM $WZq \rightarrow 3 \text{ leptons} + \text{jet} + \cancel{E}_T$	0.023	23		
SM $WZg \rightarrow 3 \text{ leptons} + \text{jet} + \cancel{E}_T$	0.0072	7.2		

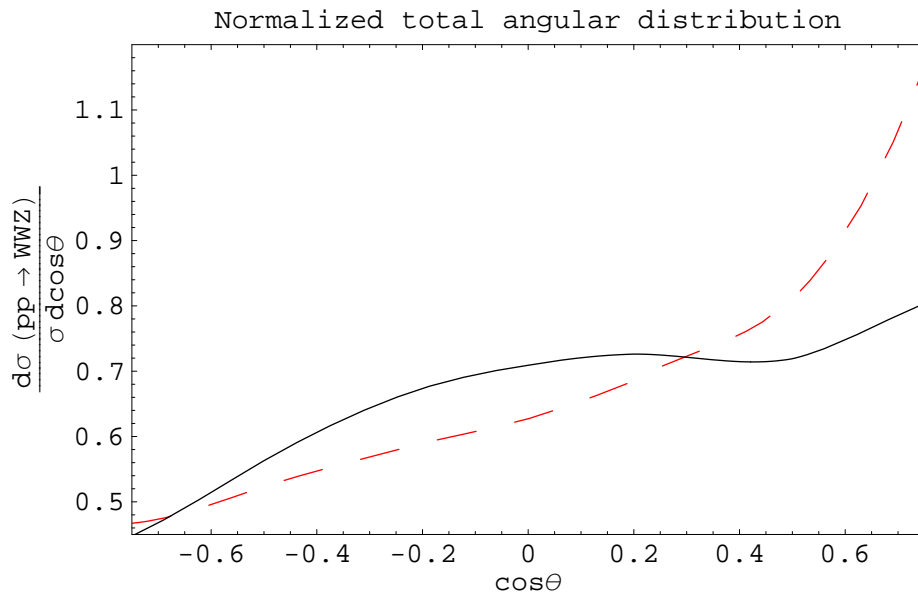


FIG. 4: Normalized total angular distribution for $\sigma(pp \rightarrow WWZ)$ cross-section for $m_1^G = 1.5 \text{ TeV}$ (solid) and $m_1^G = 2 \text{ TeV}$ (dashed) with cuts as in Eq.18 and Eq.19.

angular distribution in the graviton rest frame for all these modes. We performed angular analysis using Wigner D-matrix in order to derive the relationship between the graviton spin, angular distribution peak value, and other theoretically calculable quantities. As our method only requires to measure this peak value, where most of the signal events will be concentrated, it may be possible to achieve this goal with a relatively low sample of $O(10)$ events. In any case, our main aim in this work is to illustrate how our method can work, at least in principle. Using statistical results

of [10] for $pp \rightarrow ZZ \rightarrow 4$ leptons and our analysis of $pp \rightarrow W^{KK}W \rightarrow WWZ \rightarrow 3$ leptons + jet + \cancel{E}_T decay modes, we showed that with 1000 fb^{-1} of data, these channels allow this number of events to accumulate for the RS graviton up to ~ 2 TeV. As a byproduct of our analysis, we found that $W^{KK}(Z^{KK})W_L(Z_L)$ graviton decay modes, which have not been studied before, have a Br comparable to the zero mode decay channels as summarized in Tables.I-V. These decay modes open new channels to search for the RS gravitons. As an extra bonus, reconstruction of intermediate KK gauge bosons in these modes will be important to reveal the detailed workings of the RS model.

Acknowledgments

We thank Hooman Davoudiasl for a careful reading of the manuscript and for many useful discussions. Work of O.A. is supported in part by DOE under contract number DE-FG02-01ER41155. A.S. is supported in part by the DOE grant DE-AC02-98CH10886 (BNL).

APPENDIX A: SPIN-2 WIGNER SMALL D-MATRIX

$$\begin{aligned}
d_{22}^{(2)}(\beta) &= \frac{(1 + \cos\beta)^2}{4}, & d_{21}^{(2)}(\beta) &= -\frac{1 + \cos\beta}{2} \sin\beta, & d_{2-1}^{(2)}(\beta) &= -\frac{1 - \cos\beta}{2} \sin\beta \\
d_{20}^{(2)}(\beta) &= \frac{\sqrt{6}}{4} \sin^2\beta, & d_{2-2}^{(2)}(\beta) &= \frac{(1 - \cos\beta)^2}{4}, & d_{10}^{(2)}(\beta) &= -\sqrt{\frac{3}{2}} \sin\beta \cos\beta \\
d_{11}^{(2)}(\beta) &= \frac{1 + \cos\beta}{2} (2\cos\beta - 1), & d_{1-1}^{(2)}(\beta) &= \frac{1 - \cos\beta}{2} (2\cos\beta + 1), \\
d_{00}^{(2)}(\beta) &= \frac{3\cos^2\beta - 1}{2}.
\end{aligned} \tag{A1}$$

-
- [1] L. Randall and R. Sundrum, Phys. Rev. Lett. **83**, 3370 (1999) [arXiv:hep-ph/9905221].
 - [2] H. Davoudiasl, J. L. Hewett and T. G. Rizzo, Phys. Rev. D **63**, 075004 (2001) [arXiv:hep-ph/0006041].
 - [3] W. D. Goldberger and M. B. Wise, Phys. Rev. Lett. **83**, 4922 (1999) [arXiv:hep-ph/9907447].
 - [4] H. Davoudiasl, J. L. Hewett and T. G. Rizzo, Phys. Lett. B **473**, 43 (2000) [arXiv:hep-ph/9911262].
 - [5] A. Pomarol, Phys. Lett. B **486**, 153 (2000) [arXiv:hep-ph/9911294].
 - [6] Y. Grossman and M. Neubert, Phys. Lett. B **474**, 361 (2000) [arXiv:hep-ph/9912408].
 - [7] S. J. Huber and Q. Shafi, Phys. Lett. B **498**, 256 (2001) [arXiv:hep-ph/0010195].

- [8] T. Gherghetta and A. Pomarol, Nucl. Phys. B **586**, 141 (2000) [arXiv:hep-ph/0003129].
- [9] A. L. Fitzpatrick, J. Kaplan, L. Randall and L. T. Wang, arXiv:hep-ph/0701150.
- [10] K. Agashe, H. Davoudiasl, G. Perez and A. Soni, Phys. Rev. D **76**, 036006 (2007) [arXiv:hep-ph/0701186].
- [11] H. Davoudiasl, J. L. Hewett and T. G. Rizzo, Phys. Rev. Lett. **84**, 2080 (2000) [arXiv:hep-ph/9909255].
- [12] O. Antipin, D. Atwood and A. Soni, arXiv:0711.3175 [hep-ph].
- [13] L. T. Wang and I. Yavin, arXiv:0802.2726 [hep-ph].
- [14] K. Agashe, A. Delgado, M. J. May and R. Sundrum, JHEP **0308**, 050 (2003) [arXiv:hep-ph/0308036].
- [15] M. S. Carena, E. Ponton, J. Santiago and C. E. M. Wagner, Nucl. Phys. B **759**, 202 (2006) [arXiv:hep-ph/0607106].
- [16] S. Chang, C. S. Kim and J. Song, JHEP **0702**, 087 (2007) [arXiv:hep-ph/0607313].
- [17] K. Agashe, A. E. Blechman and F. Petriello, Phys. Rev. D **74**, 053011 (2006) [arXiv:hep-ph/0606021].
- [18] S. Chang, C. S. Kim and J. Song, arXiv:0712.0207 [hep-ph].
- [19] K. Agashe, G. Perez and A. Soni, Phys. Rev. Lett. **93**, 201804 (2004) [arXiv:hep-ph/0406101].
- [20] G. Burdman, Phys. Lett. B **590**, 86 (2004) [arXiv:hep-ph/0310144].
- [21] K. Agashe, G. Perez and A. Soni, Phys. Rev. D **75**, 015002 (2007) [arXiv:hep-ph/0606293]; P. J. Fox, Z. Ligeti, M. Papucci, G. Perez and M. D. Schwartz, arXiv:0704.1482 [hep-ph];
For other study of FCNC's in such models see K. Agashe, M. Papucci, G. Perez and D. Pirjol, arXiv:hep-ph/0509117.
- [22] That LR operators cause enhanced contributions to $\Delta S = 2$ processes was first pointed out in, G. Beall, M. Bander and A. Soni, Phys. Rev. Lett. **48**, 848 (1982).
- [23] M. Bona *et al.* [UTfit Collaboration], arXiv:0707.0636 [hep-ph].
- [24] K. Agashe *et al.*, arXiv:0709.0007 [hep-ph].
- [25] C. Csaki, A. Falkowski and A. Weiler, arXiv:0804.1954 [hep-ph].
- [26] G. Moreau and J. I. Silva-Marcos, JHEP **0603**, 090 (2006) [arXiv:hep-ph/0602155].
- [27] A. L. Fitzpatrick, G. Perez and L. Randall, arXiv:0710.1869 [hep-ph].
- [28] K. Agashe, G. Perez and A. Soni, Phys. Rev. D **71**, 016002 (2005) [arXiv:hep-ph/0408134].
- [29] H. Davoudiasl, G. Perez and A. Soni, arXiv:0802.0203 [hep-ph].
- [30] See R. Sundrum talk at the "Brookhaven Forum 2007: New Horizons at Colliders", May 2007.
- [31] S. U. Chung, "SPIN FORMALISMS," CERN-71-08; Lectures given in the Academic Training Program of CERN 1969-1970.
- [32] S. M. Berman and M. Jacob, Phys. Rev. **139**, B1023 (1965).
- [33] A. Pukhov *et al.*, arXiv:hep-ph/9908288, E. Boos *et al.* [CompHEP Collaboration], Nucl. Instrum. Meth. A **534**, 250 (2004) [arXiv:hep-ph/0403113].
- [34] J. Pumplin, D. R. Stump, J. Huston, H. L. Lai, P. Nadolsky and W. K. Tung, JHEP **0207**, 012 (2002) [arXiv:hep-ph/0201195].
- [35] S. C. Park, H. S. Song and J. H. Song, Phys. Rev. D **65**, 075008 (2002) [arXiv:hep-ph/0103308].

- [36] F. Gianotti *et al.*, Eur. Phys. J. C **39**, 293 (2005) [arXiv:hep-ph/0204087].
- [37] See also H. U. Bengtsson, W. S. Hou, A. Soni and D. H. Stork, Phys. Rev. Lett. **55**, 2762 (1985).
- [38] R. Contino, Y. Nomura and A. Pomarol, Nucl. Phys. B **671**, 148 (2003) [arXiv:hep-ph/0306259].
- [39] K. Agashe, R. Contino and A. Pomarol, Nucl. Phys. B **719**, 165 (2005) [arXiv:hep-ph/0412089].
- [40] L.March, E.Ros, M.Vos, “Signatures with multiple b-jets in the Left-Right twin Higgs model - fast simulation study of the ATLAS reach,” talk presented at the Les Houches BSM working group, Twin Higgs discussion session, 23rd June, 2007.